Journal of Renewable Materials

Tech Science Press

DOI: 10.32604/jrm.2021.015624

ARTICLE

Corrosion Protection of 5083 AA in Saline Water by Polyacrylonitrile Nanofibers

Enas H. Ali, Juman A. Naser*, Zainab W. Ahmed and Taki A. Himdan

Department of Chemistry, College of Education for Pure Science-Ibn Al-Haitham, University of Baghdad, Baghdad, Iraq

*Corresponding Author: Juman A. Naser. Email: drjumannaser@gmail.com; juman.a.n@ihcoedu.uobaghdad.edu.iq

Received: 31 December 2020 Accepted: 04 March 2021

ABSTRACT

Polymeric nanofibers are a promising technology to protect the metal surfaces from corrosion. Through the literature search, the use of polyacrylonitrile nanofibres (PANNFs) as a corrosion inhibitor coating for aluminum alloys has not been evaluated. This work includes the development of a new, lightweight, high surface area and efficient coating of PANNFs that produced using electrospinning process to resist the corrosion of aluminum alloys (AA5083) which immersed in 0.6 M NaCl at alkaline medium (pH = 12) and acidic medium (pH = 1) at a range of temperatures (293–323) K. The PANNFs coating was successfully deposited on AA 5083 specimens, where these samples were considered as a collector electrode in the electrospinning process. The corrosion experiments of the aluminum alloys coated with PANNFs before and after immersion in both corrosive mediums were investigated using cyclic potential polarization (CPP). The results confirmed that the PANNFs coating was able to protect the surface of the aluminum specimens from corrosion, by reducing the corrosion current and increasing the surface polarization resistance, thus reducing the corrosion rate. The protection efficiency was found in the alkaline medium 98.8% while in the acidic medium 83.3%. So, it was in both mediums decreased with the increase in temperature. The shape, distribution and size of the polymeric nanofibers that formed the coating were also examined using field emission scanning electron microscopy (FE-SEM) and the percentages of the structural components of these fibers were detected using the X-ray dispersion spectroscopy (EDS). The surface of aluminum specimens was completely covered by PANNFs. These electrospun nanofibers have worn out and lined up spacing after immersion in the corrosive mediums. The diameters average of PANNFs was found to be about 200 and 150 nm before and after immersion, respectively.

KEYWORDS

Corrosion protection; nanofibers; polyacrylonitrile; aluminum alloy; saline medium; protection efficiency

1 Introduction

Metallic materials are widely used for a wide variety of industrial applications and emerging alloys were already produced to best suit the specifications for a particular application. The methods of surface engineering developing also made possible a range of surface treatments or coatings to increase the resistance of corrosion for metallic materials. For this reason, conventional methods such as electrodeposition [1], electrochemical coating [2], chemical conversion [3] and anodizing [4] have become the most commonly used, while others include the use of chromates, which pose a significant hazard to the environment and human health.

The promising alternative for this purpose is the ability to develop and modify materials at the nano-scale, as the ability to incorporate nanometric-scale features on the materials will improve the ratio of surface to volume and offer advanced functionalities.

Aluminum alloys (AA) are commonly used in several products as their low density and cost in addition to high thermal and electrical conductivity. These benefits make them useful in diverse fields, such as transportation, food processing, scrubbers, electronics, petroleum heat exchangers, storage tanks and marine applications [5–8]. In general, aluminum forms a transparent protective passive oxide layer on its surface when exposed to an aqueous solution. Because of the high solubility of this oxide film does not give adequate protection against both acidic and alkaline environments that increases the corrosion rate.

Any coaters, such as polymers, organic and inorganic materials have been used to mitigate electrochemical aluminum corrosion by isolating its surface from the medium of corrosion by creating a resistant layer of oxide on the metal surface [9–11].

Electrospinning was chosen as the manufacturing technique for the nanofibers coting on aluminum substrates. It is a simple and flexible deposition technique that uses the electrostatic forces to create very fine polymeric fibers in nano-scale [12]. Moreover, this method is a very effective instrument for the manufacture of high surface area materials [13]. Hence, electrospun nanofibres (ENFs) can be composed of various polymer forms, such as natural [14], synthetic [15] and copolymer [16]. Nanofibers have diverse applications in three main areas; water treatment, biomedical care and energy generation or storage that represented in photocatalysis, ultrafiltration, drug delivery, wound dressing, tissue engineering, solar cells, batteries, supercapacitors and fuel cells [17].

Aluminum electrochemical corrosion was examined by Sherif et al. using cyclic potentiodynamic polarization (CPP) and electrochemical impedance spectroscopy (EIS) measurements in freely aerated stagnant solutions of 3.5 wt% NaCl with and without coatings of polyvinyl alcohol nanofibers (PVANFs) and polyvinyl chloride nanofibers (PVCNFs). The deposited nanofibers coatings have been found to minimize the currents and rate of corrosion as well as improve the aluminum corrosion resistance in NaCl solution [18]. Firouzi et al. succeeded in protection of the aluminum alloy 6082 that immersed in 3.5 wt% NaCl medium against corrosion utilizing electrospinning technique, by coating it with nanofibers of crosslinked polyvinyl alcohol (PVANFs). A significant resistance of corrosion of approximately 26 kX with reference to the alloy of blank (about 3.8 kX) was reported after 270 h [19].

Moreover, the hydrophobic property can improve the protection against corrosion. Li et al. demonstrated the use of polystyrene nanofibers (PSNFs) which are superior hydrophobic to protect an aluminum mesh, and the results of the cyclic potentiodynamic polarization (CPP) showed that the coating is highly resistant in 3.5 wt% NaCl aqueous solution [20]. Cui et al. reported the great potential of highly hydrophobic surfaces *vs.* corrosion, where electrospun nanofibers of polyvinylidenefluoride (PVDF)/stearic acid (SA) that was characterized by their superior anti-corrosion performances of aluminum alloy even after immersion in aqueous solutions of 3.5 wt% NaCl for 30 days [21].

According to our knowledge, no work carried out on the efficiency investigation of polyacrylonitrile nanofibers coating in corrosion inhibition of aluminum alloys. Thus, the influence of PANNFs coating on the activity of 5083 AA corrosion using cyclic potentiodynamic polarization method in a medium of 0.6 M NaCl at acidic medium pH = 1 and alkaline medium pH = 12 was studied in the current research. The coated aluminum surface with PANNFs were characterized before and after immersing in corrosive solutions utilizing field emission scanning electron microscope (FE-SEM) and X-ray dispersion spectroscopy (EDS).

2 Experimental

2.1 Materials

Hydrochloric acid HCl, potassium hydroxide KOH and sodium chloride NaCl were obtained from BDH. Polyacrylonitrile $(C_3H_3N)n$ and dimethylformamide (DMF) were supplied from Sigma Aldrich.

2.2 Corrosive Medium

Double distilled water has been used in all preparations of the corrosive mediums. All measurements were performed in a saline aqueous solution containing 0.6 M NaCl which has a comparable level to that of seawater at acidic medium pH = 1 and alkaline medium pH = 12 using aqueous solution of 0.1 M HCl and 0.01 M KOH, respectively.

2.3 Aluminum Alloy Specimens

The corrosion experiments were performed on 5083 aluminium alloy specimens of the following composition (weight %): 4.5 Mg, 0.50 Mn, 0.40 Fe, 0.40 Si, 0.20 Cr, 0.25 Zn, 0.10 Cu and balance Al. The aluminum plate was cut into a circular shape with a diameter 2 cm and thickness 2 mm. Before immersing in the corrosive solutions, the specimens surfaces were abraded using various grades of emery paper (200, 400, 800, 1200 and 2000), then rinsed by acetone and washed by distilled water, and dried with a cloth, finally kept in a desiccator. The exposed surface area to the aggressive medium was 1 cm^2.

2.4 Electrospining Process

The electrospinning solution of polyacrylonitrile 4% w/v was prepared by dissolving its granules in DMF with a continuous stirring for 240 min at a temperature 50°C until a homogeneous solution was obtained, as in a similar way to previous work [22]. The electrospinning process was carried out under a pressure 25 kV, PAN solution was extruded through a nozzle 0.9 mm at a velocity rate 0.02 mL/min towards the aluminum alloy species that were fixed on the collector electrode at a distance 0.15 m. The coated alloys with PANNFs were dried in a vacuum oven for 120 min at 80°C to get rid of the solvent residue. The coated alloys specimens are showed in Fig. 1.

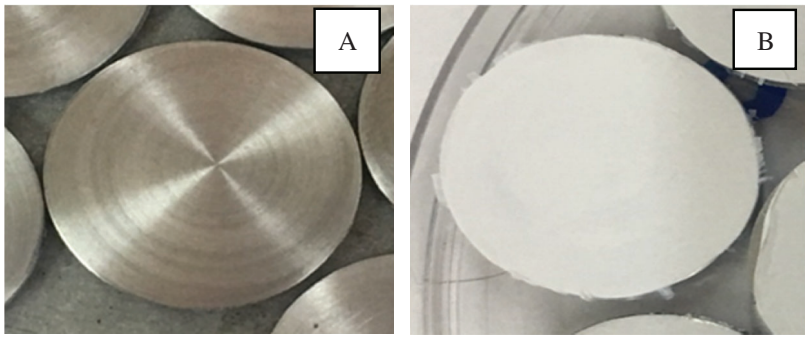

Figure 1: Photograph of 5083 AA specimen: A; uncoated and B; coated by PANNFs

2.5 Cyclic Potentiodynamic Polarization Measurements

The cyclic potentiodynamic polarization measurements were conducted using Wenking M lab potentiostat in a conventional three-electrode glass cell double-wall pyrex glass with working volume 1L capacity. A three-electrode configuration was used that consists of the studied sample (1.5 cm^2) as a working electrode, a saturated Ag/AgCl reference electrode and a platinum counter electrode. After steady-state potential was identified in the cathodic or anodic direction and a potential from −200 mV to + 200 mV, the polarization measurements were carried out at a scan rate of 2 mV/s. All measurements were performed in 0.6 M NaCl medium at pH = 1 and pH = 12 in a presence and absence of the coating layer of PANNFs. Each experiment was conducted at least twice and the results were reproducible.

3 Results and Discussion

3.1 Surface Morphology Analysis

3.1.1 FE-SEM Analysis

The analysis of (FE-SEM) has been performed by a field emission scanning electron microscope (ZEISS ZEISS SIGMA VP) to investigate the morphology, structure and distribution of the coated 5083 AA surface with PANNFs (Fig. 2). The coated alloys surface were examined before and after the immersion in 0.6 M NaCl medium at pH = 1 and pH = 12. In comparing these surfaces before and after the corrosion tests, it can be seen that the PANNFs have worn out and lined up spacing than they were before the immersion, while the surface of aluminum specimens was completely covered by nanofibers. This conclusion means that the solution of NaCl has reached to parts of the alloy surface. The micrograph of FE-SEM also shows that the change in the surface appearance of the coated aluminum specimen immersed in pH = 12 is less compared to pH = 1. It was also found that the fibers diameter average of PANNFs was about 200 nm ± 50 before immersion, while it became 150 nm ± 50 after the immersion in both corrosive mediums. Also, there is a decrease in the thickness of nanofibres and the surface erosion of aluminum alloy in some areas. Additionally to a presence of clusters aggregation of salt on their grid after the exposure to the saline solutions. This may be attributed to the pH enhancing the molecular interactions between the corrosive products and PANNFs [23].

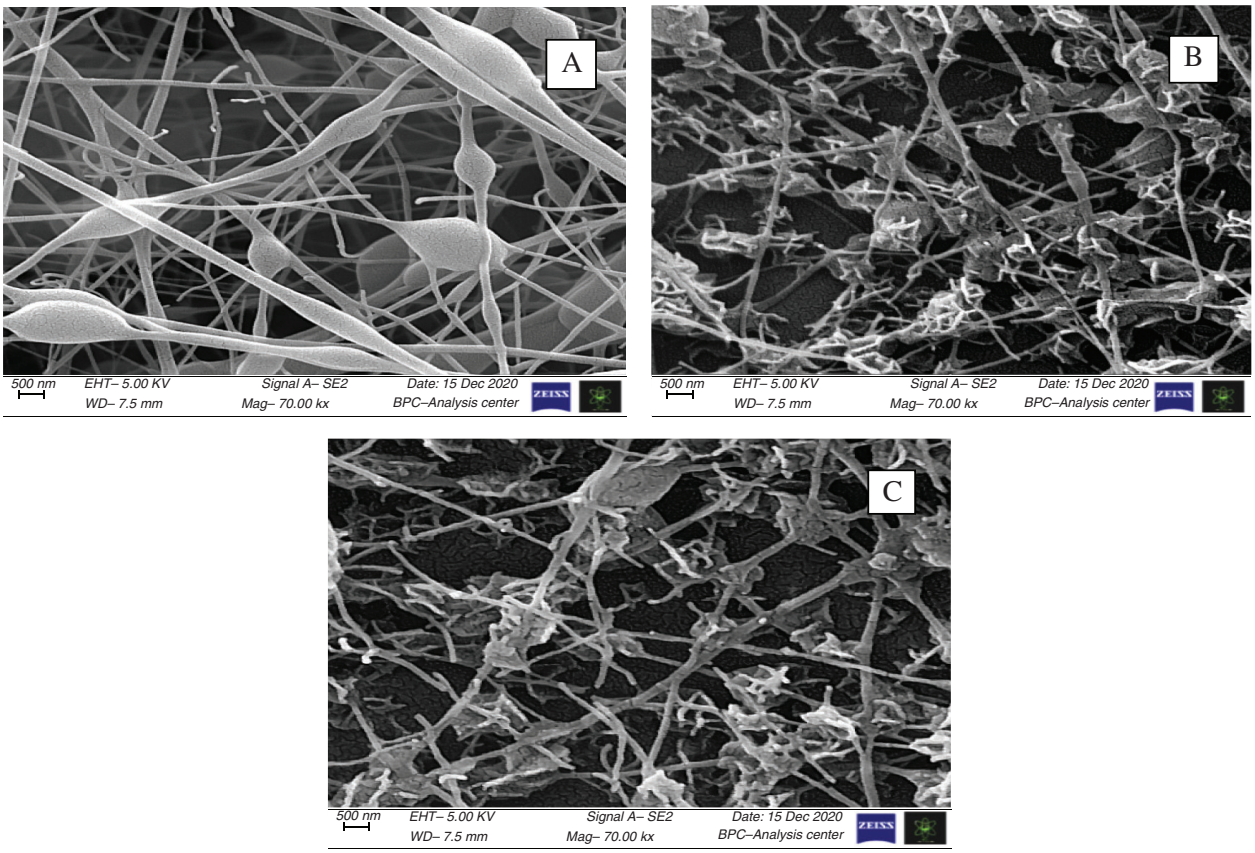

Figure 2: FE-SEM micrograph of the coated 5083 AA surface by PANNFs: (A) before the immersion in 0.6 M NaCl medium, (B) after the immersion in 0.6 M NaCl medium at pH = 1 and (C) after the immersion in 0.6 M NaCl medium at pH = 12

3.1.2 EDS Analysis

The analysis of EDS was conducted by an energy dispersive spectrometer (Oxford Instru EDS X-MAX-80) to evaluate the elements weight percentage of the coated 5083 AA surface with PANNFs before and after the immersion in 0.6 M NaCl at pH = 1 and pH = 12, Fig. 3. It shows the presence of carbon and nitrogen as major components of PANNFs. So, it is noticed that the percentage of elements was close together before and after immersion in the corrosive medium. All spectrums had a small peak approximately at 1.1 keV attributed to coat the sample with a thin layer of gold as a requirement for FE-SEM and EDS techniques.

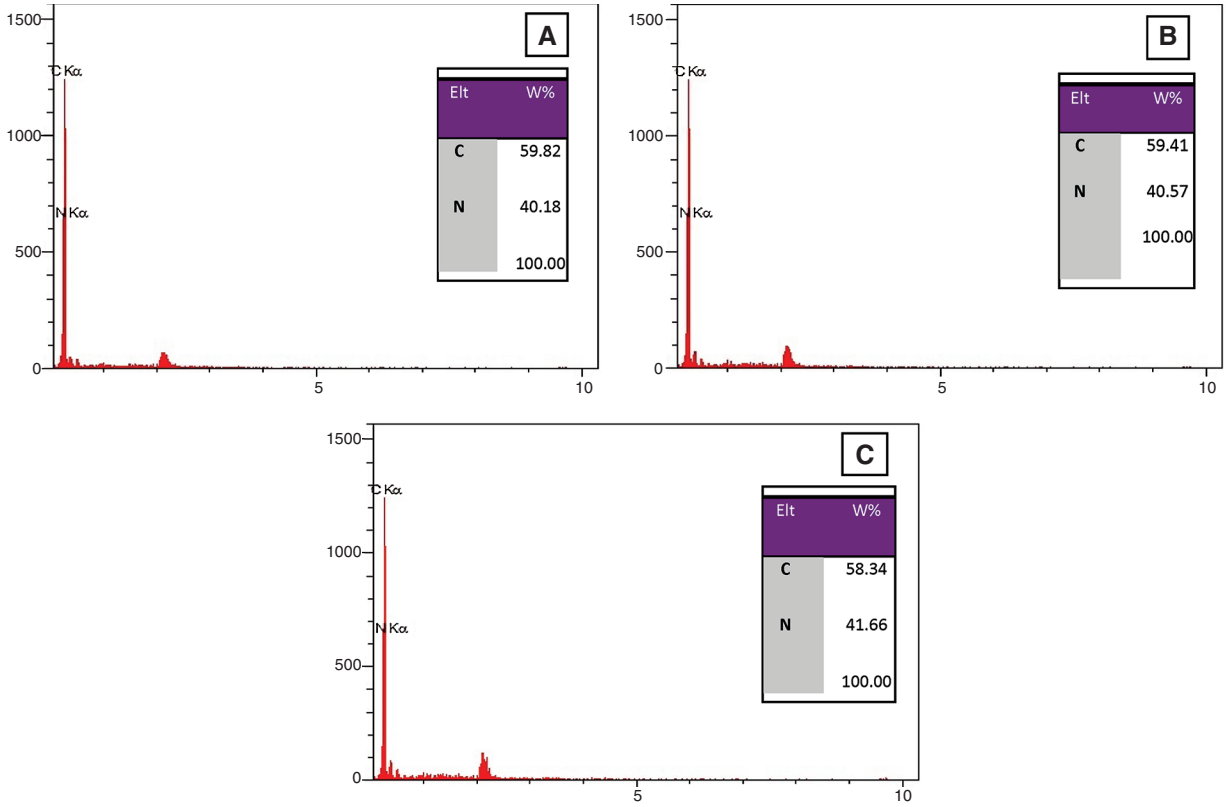

Figure 3: EDS spectrum and elements weight percentages of the coated 5083 AA surface by PANNFs: A; before the immersion in 0.6 M NaCl medium, B; after the immersion in 0.6 M NaCl medium at pH = 1 and C; after the immersion in 0.6 M NaCl medium at pH = 12

3.2 Polarization Curves

Figs. 4–7 show the polarization curves of anodic and cathodic for uncoated and coated 5083 AA with PANNFs in 0.6 M NaCl at pH = 1 and 12, respectively in the range of temperatures (293–323)K. Tafel extrapolation method was used to calculate the corrosion parameters (E_{corr}), (i_{corr}) (b_c) and (b_a) from the polarization curves.

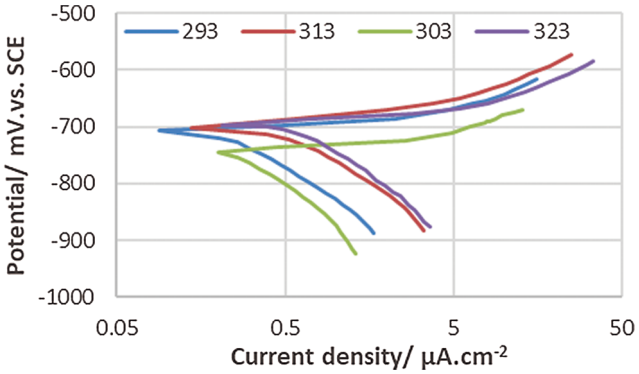

Figure 4: Polarization behavior of corrosion of the uncoated 5083 AA and immersed in 0.6 M NaCl medium at pH = 1

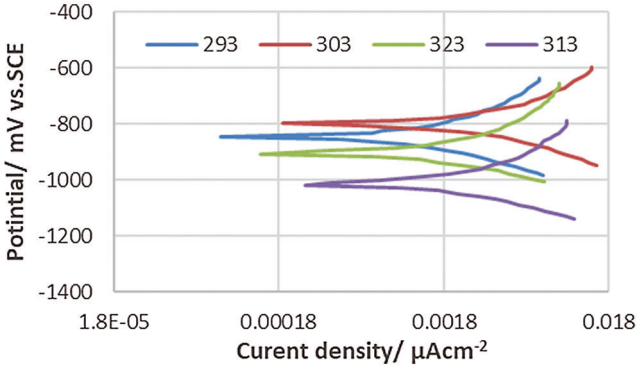

Figure 5: Polarization behavior of corrosion of the uncoated 5083 AA and immersed in 0.6 M NaCl medium at pH = 12

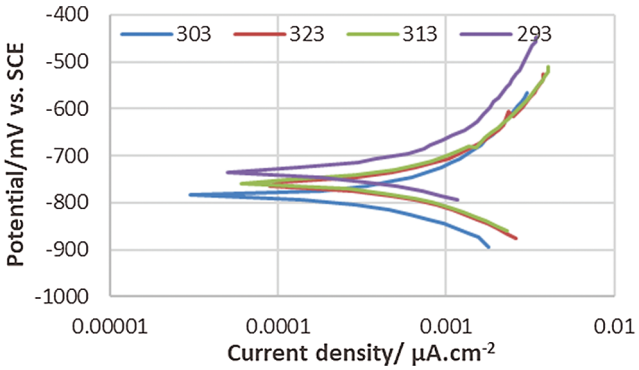

Figure 6: Polarization behavior of corrosion of the coated 5083 AA and immersed in 0.6 M NaCl medium at pH = 1

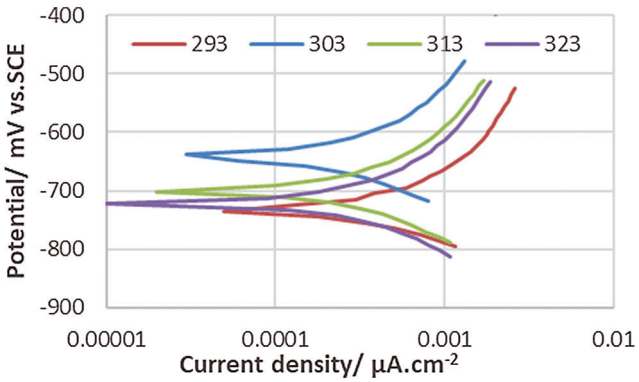

Figure 7: Polarization behavior of corrosion of the coated 5083 AA and immersed in 0.6 M NaCl medium at pH = 12

The experimental data are displayed in Tabs. 1 and 2. These data show with increasing temperature, the corrosion current density (i_{corr}) increases. Thus, the corrosion potential (E_{corr}) nearly becomes more negative with increasing temperature. It is obvious from the results of potentiodynamic which listed in Tabs. 1 and 2 that the coating layer of PANNFs decreased the corrosion rate in different mediums, as a result to the coverage of the specimens surface. The values changes of Tafel constants refer to the inhibition effect of the electrospun nanofibers coating which dominates the reactions of anodic and cathodic compared to the uncoated aluminum alloy, as it is consistent with the obtained result in reference [24].

Table 1: Data of polarization behavior of corrosion of the uncoated and coated 5083 AA that immersed in 0.6 M NaCl medium at pH = 1 and a range of temperature (293–323) K

	T/K	Corrosion		b		Weight loss/g.m^{-2}.d^{-1}	Penetration loss/mm.year^{-1}
		E_{corr}/mV	i_{corr}/µA.cm^{-2}	$-b$/mV decade^{-1}	$+b$/mV decade^{-1}		
Uncoated	293	744	125.85	444.5	41.4	1.01×10^{-1}	1.37
	303	709	235.68	508	23.1	1.9×10^{-1}	2.56
	313	709.8	290	285.3	24.4	2.4×10^{-1}	3.16
	323	711.9	318.14	139.8	20.8	2.56×10^{-1}	3.46
Coated	293	714	20..99	60.2	20.2	1.69×10^{-1}	2.28
	303	713.4	44.01	106.5	22.8	3.54×10^{-1}	4.79
	313	701.7	61.99	138.6	17.6	4.99×10^{-1}	6.74
	323	706	76.43	137.1	12	6.15×10^{-1}	8.31

Table 2: Data of polarization curve for corrosion of the uncoated and coated 5083 AA that immersed in 0.6 M NaCl medium at pH = 12 and a range of temperature (293–323) K

	T/K	Corrosion		b		Weight loss/g.m^{-2}.d^{-1}	Penetration loss/mm.year^{-1}
		E_{corr}/mV	i_{corr}/µA.cm^{-2}	−b/mV decade^{-1}	+b/mV decade^{-1}		
Uncoated	293	1382.8	77.20	52.4	114.2	6.21×10^{-1}	8.4
	303	1394.8	128.23	69.8	81	1.03×10^{-1}	1.39
	313	1388	151.48	59.6	106	1.22×10^{-1}	1.65
	323	1399	155.51	78.1	3.70	1.20×10^{-1}	1.69
Coated	293	1331.7	1.04	168.8	130.9	8.33×10^{-1}	1.13
	303	1229	13.97	185	62.2	1.12×10^{-1}	1.52
	313	1222.3	18.46	95.8	334.7	1.49×10^{-1}	2.01
	323	1361.7	38.87	50.6	59.3	3.13×10^{-1}	4.23

3.3 Kinetic Parameters

The temperature has a significant impact on the rate of electrochemical corrosion of metals as in the majority of chemical reactions, it is the accelerating factor. It enhances the reacted species energy, resulting in a much faster chemical reaction. From Tabs. 1 and 2 we found that the values of i_{corr} increases with temperature increasing and protection efficiency decreases with temperature increasing.

Arrhenius equation was used to calculate activation energy for corrosion of uncoated and coated 5083 AA by PANNFs in alkaline and acidic mediums, as shown expression [25]:

$$\ln\left(i_{corr}\right) = \ln A - E_a^*/RT \quad (1)$$

where, A is the pre-exponential factor, E_a* is the energy of activation, R is the gas constant and T is the temperature in Kelvin. Eq. (1) predicts that plotting of *ln* (i_{corr}) against *1/T* that should be linear as experimentally observed in Figs. 8 and 9.

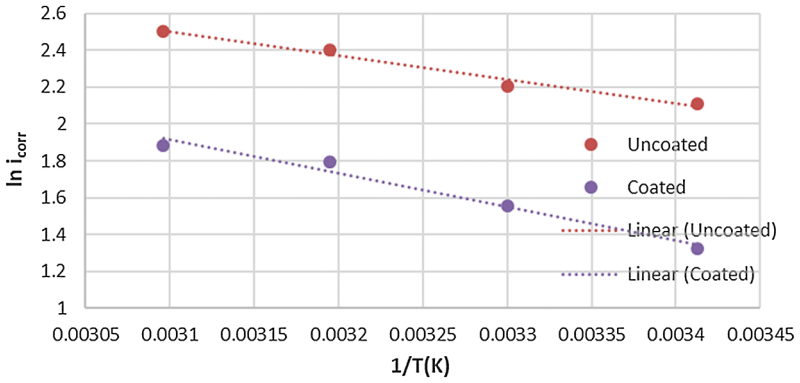

Figure 8: Arrhenius plot for corrosion of the uncoated and coated 5083 AA that immersed in 0.6 M NaCl medium at pH = 1 and a range of temperature (293–323) K

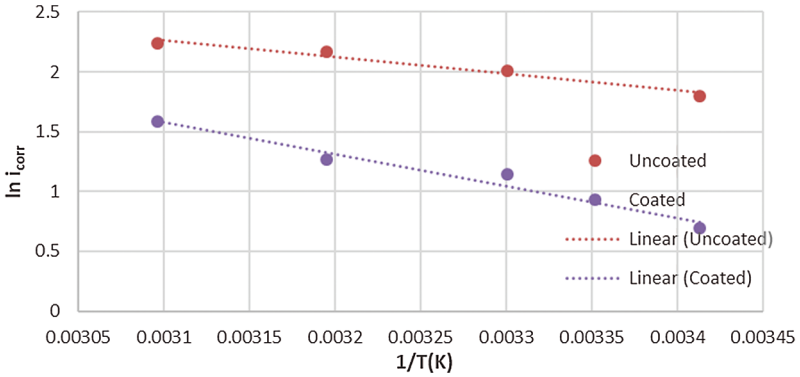

Figure 9: Arrhenius plot for corrosion of the uncoated and coated 5083 AA that immersed in 0.6 M NaCl medium at pH = 12 and a range of temperature (293–323) K

The slope of line represents (*–Ea*/RT)*, whereas the intercept expresses *ln A*. The activation entropy ΔS* was culculated from the A value utilizing the following equation [26]:

$$A = k_B T/h \exp(\Delta S^*/R) \quad (2)$$

where k_B is Boltzmann's constant, h is Planck's constant and T is the absolute temperature of the medium.

The estimated values of E_a* and ΔS* are abstracted in Tabs. 3 and 4. It was noticed that E_a* values was increase for 5083 AA after coating with PANNFs in alkaline and acidic medium. The entropy of activation ΔS* values are negative that suggests there is an association rather than dissociation in the rate determining step. This implies that the activated complex is in higher-order state than the initial state [27].

Table 3: Activation value of energy (E_a*) and entropy (ΔS*) for corrosion of the uncoated and coated 5083 AA that immersed in 0.6 M NaCl medium at pH = 1

	E_a*/kJ.mol^{-1}	-ΔS*/J.K^{-1}.mol^{-1}	A/molecule m^{-2}.S^{-1}
Uncoated	24.76	123.33	3.2255x10^6
Coated	34.98	103.02	3.7836x10^7

Table 4: Activation value of energy (Ea*) and entropy (ΔS*) for corrosion of the uncoated and coated 5083 AA that immersed in 0.6 M NaCl medium at pH = 12

	E_a*/kJ.mol^{-1}	-ΔS*/J.K^{-1}.mol^{-1}	A/molecule m^{-2}.S^{-1}
Uncoated	26.76	121.64	3.9609x10^6
Coated	50.84	60.65	6.418x10^9

3.4 Thermodynamic Parameters

The values of enthalpy ΔH° and entropy ΔS° for the corrosion of the uncoated and coated 5083 AA by PANNFs that immersed in 0.6 M NaCl medium have been estimated according the following relation [28]:

$$i_{corr} = RT/Nh \exp(\Delta S^\circ) \exp(-\Delta H^\circ/RT) \quad (3)$$

where h is Plank's constant, N is Avogadro's number, ΔS° is the entropy and ΔH° is the enthalpy. Figs. 10 and 11 show a plot of ($ln\ i_{corr}/T$) versus $1/T$. Hence, the values of ΔH° and ΔS° can be obtained from the slope and intercept of the straight, respectively.

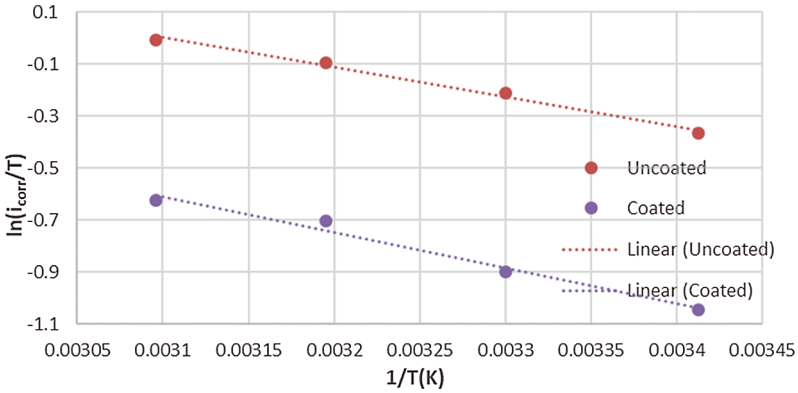

Figure 10: Plot of ln (i_{corr} /T) against $1/T$ for corrosion of the uncoated and coated 5083 AA that immersed in 0.6 M NaCl medium at pH = 1

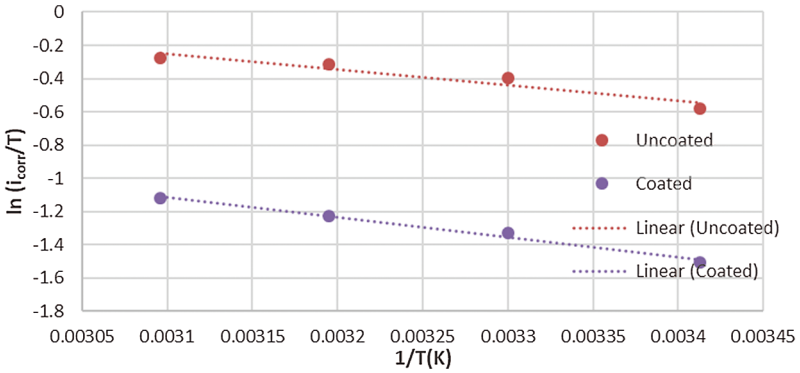

Figure 11: Plot of ln (i_{corr}/T) against 1/T for corrosion of the uncoated and coated 5083 AA that immersed in 0.6 M NaCl medium at pH = 12

The protection efficiency values *(PE%)* were calculated according to the following equation [29] and listed in Tab. 5.

$$PE\% = [((i_{corr})\text{uncoated} - (i_{corr})\ \text{coated})/(i_{corr})\text{uncoated}] \times 100 \quad (4)$$

where (i_{corr}) uncoated and (i_{corr}) coated are corrosion current densities for uncoated and coated 5083 AA by PANNFs, respectively. The coated specimens showed good enhancing against corrosion, and the maximum value of efficiency was found to be 98.6 in basic medium and 83.3 in acidic medium.

Table 5: Surface coverage, protection efficiency and thermodynamic parameters for corrosion of the uncoated and coated 5083 AA that immersed in 0.6 M NaCl medium at pH = 1 and pH = 12

Surface condition	*T*/K	θ	*PE*%	$-\Delta G°$/kJ.mol^{-1}	$-\Delta H°$/kJ.mol^{-1}	$-\Delta S°$/kJ.mol^{-1}.K^{-1}
Uncoated pH = 1	293	_	_	97.16	22.925	253.37
	303	_	_	99.69		
	313	_	_	102.20		
	323	_	_	104.76		
Coated pH = 1	293	0.833	83.3	100.05	26.273	251.8
	303	0.813	81.3	102.56		
	313	0.789	78.9	105.08		
	323	0.764	76.4	107.6		
Uncoated pH = 12	293	_	_	89	17.988	242.36
	303	_	_	91.42		
	313	_	_	93.85		
	323	_	_	96.27		
Coated pH = 12	293	0.986	98.6	93.27	22.775	240.6
	303	0.890	89.0	95.67		
	313	0.878	87.8	98.08		
	323	0.75	75	100.48		

The calculated values ΔG°, ΔS° and ΔH° that are summarized in Tab. 5. The entropy values ΔS° for uncoated and coated 5083 AA are negative implying that there was the association of PANNFs rather than dissociation. The negative values of ΔH° demonstrate that corrosion is an exothermic process [30]. Thermodynamically, ΔG° were associated with the standard enthalpy ΔH° and standard entropy ΔS° according to the following express [31]:

$$\Delta G^{\circ} = \Delta H^{\circ} - T\Delta S^{\circ} \quad (5)$$

ΔG° values for uncoated and coated 5083 AA in acidic and basic medium were negative suggesting spontaneously of the corrosion process [11]. Therefore, the ΔG° values of coated specimens are higher than those of uncoated, which means the PANNFs coating increase the resistance of aluminum alloys surface against corrosion.

It has been found that PANNFs coating reduces the current and corrosion rate of aluminum 5083 in a solution of 0.6 M NaCl at an acidic and basic medium, thus electrospining is a preferred technique compared to conventional techniques. Therefore, it is possible to protect the aluminium surfaces of cans food, pipes and tanks from corrosion by coating them with nanofibers.

4 Conclusions

The effect of the PANNFs coating on the corrosion behavior of 5083 AA specimens immersed in alkaline medium (pH = 12) KOH and acidic medium (pH = 1) of HCl that containing a concentration of 0.6 M NaCl was studied using cyclic potential polarization (CPP) at a range of temperatures (293–323) K. The surface morphology of the produced nanofibres coating before and after immersion in corrosive solution at pH = 1 and pH = 12 was examined using a scanning electron microscopy (FE-SEM), and the average of diameter nanofibers was about 200 and 150 nm before and after immersion in corrosive mediums, respectively. The results of the cyclic potential polarization showed that the coated aluminum surface by PANNFs reduces the corrosion rate due to decrease of the corrosion current value and increase of the polarization resistance value of compared to the uncoated surface. The measurements also exhibited that the corrosion rate in the alkaline medium is less than that in the acidic medium. In general, all results confirmed that coating the aluminum alloy surface by PANNFs could protect it from corrosion in saline water. Thus, the use of electrospining has proven to be a promising coating technique to protect aluminium against corrosion in marine environments and heat exchangers units.

Acknowledgement: The authors extend their acknowledgement to the Deanship of College of Education for Pure Science-Ibn Al-Haitham at University of Baghdad for supporting this research.

Funding Statement: The authors received no specific funding for this study.

Conflicts of Interest: The authors declare that they have no conflicts of interest to report regarding the present study.

References

1. Maniam, K. K., Paul, S. (2020). Progress in electrodeposition of zinc and zinc nickel alloys using ionic liquids. *Applied Sciences, 10(15),* 5321–5341. DOI 10.3390/app10155321.
2. Al-Amiery, A. A., Ahmed, M. H. O., Abdullah, T. A., Gaaz, T. S., Kadhum, A. A. H. (2018). Electrochemical studies of novel corrosion inhibitor for mild steel in 1 M hydrochloric acid. *Results in Physics, 9,* 978–981. DOI 10.1016/j.rinp.2018.04.004.
3. Duan, G., Yang, L., Liao, S., Zhang, C., Lu, X. et al. (2018). Designing for the chemical conversion coating with high corrosion resistance and low electrical contact resistance on AZ91D magnesium alloy. *Corrosion Science, 135,* 197–206. DOI 10.1016/j.corsci.2018.02.051.

4. Usman, B. J., Scenini, F., Curioni, M. (2020). Corrosion testing of anodized aerospace alloys: Comparison between immersion and salt spray testing using electrochemical impedance spectroscopy. *Journal of the Electrochemical Society, 167(4),* 041505. DOI 10.1149/1945-7111/ab74e3.
5. Varshney, D., Kumar, K. (2020). Application and use of different aluminium alloys with respect to workability, strength and welding parameter optimization. *Ain Shams Engineering Journal, 12(1),* 1143–1152. DOI 10.1016/j.asej.2020.05.013.
6. Berlanga-Labari, C., Biezma-Moraleda, M. V., Rivero, P. J. (2020). Corrosion of cast aluminum alloys: A review. *Metals, 10(10),* 1384. DOI 10.3390/met10101384.
7. Sun, Y., Zhao, D., Song, J., Wang, C., Zhang, Z. et al. (2019). Rapid fabrication of superhydrophobic high-silicon aluminum alloy surfaces with corrosion resistance. *Results in Physics, 12,* 1082–1088. DOI 10.1016/j.rinp.2018.12.090.
8. Vasu, A., Hagos, F. Y., Noor, M. M., Mamat, R., Azmi, W. H. et al. (2017). Corrosion effect of phase change materials in solar thermal energy storage application. *Renewable and Sustainable Energy Reviews, 76,* 19–33. DOI 10.1016/j.rser.2017.03.018.
9. Bandeira, R. M., van Drunen, J., Garcia, A. C., Tremiliosi-Filho, G. (2017). Influence of the thickness and roughness of polyaniline coatings on corrosion protection of AA7075 aluminum alloy. *Electrochimica Acta, 240,* 215–224. DOI 10.1016/j.electacta.2017.04.083.
10. Xhanari, K., Finsgar, M. (2019). Organic corrosion inhibitors for aluminum and its alloys in chloride and alkaline solutions: A review. *Arabian Journal of Chemistry, 12(8),* 4646–4663. DOI 10.1016/j.arabjc.2016.08.009.
11 Ahmed, Z. W., Naser, J. A., Farooq, A. (2020). Inhibition of aluminum alloy 7025 in acid solution using sulphamethoxazole. *Egyptian Journal of Chemistry, 63(10),* 3703–3711. DOI 10.21608/EJCHEM.2020.15541.1942.
12. Xue, J., Wu, T., Dai, Y., Xia, Y. (2019). Electrospinning and electrospun nanofibers: Methods, materials, and applications. *Chemical Reviews, 119(8),* 5298–5415. DOI 10.1021/acs.chemrev.8b00593.
13. Naser, J. A., Himdan, T. A., Ibraheim, A. J. (2017). Adsorption kinetic of malachite green dye from aqueous solutions by electrospun nanofiber Mat. *Oriental Journal of Chemistry, 33(6),* 3121–3129. DOI 10.13005/ojc/330654.
14. Zhang, C., Li, Y., Wang, P., Zhang, H. (2020). Electrospinning of nanofibers: Potentials and perspectives for active food packaging. *Comprehensive Reviews in Food Science and Food Safety, 19(2),* 479–502. DOI 10.1111/1541-4337.12536.
15. Duan, G., Liu, S., Hou, H. (2018). Synthesis of polyacrylonitrile and mechanical properties of its electrospun nanofibers. *e-Polymers, 18(6),* 569–573. DOI 10.1515/epoly-2018-0158.
16. Fendi, W. J., Naser, J. A. (2018). Adsorption isotherms study of methylene blue dye on membranes from electrospun nanofibers. *Oriental Journal of Chemistry, 34(6),* 2884–2894. DOI 10.13005/ojc/340628.
17. Lim, C. T. (2017). Nanofiber technology: Current status and emerging developments. *Progress in Polymer Science, 70,* 1–17. DOI 10.1016/j.progpolymsci.2017.03.002.
18. Sherif, E. M., Es-saheb, M., El-Zatahry, A., Kenawyand, E., Alkaraki, A. S. (2012). Coating electrospun polyvinyl alcohol and polyvinyl chloride fibers as corrosion passivation applications. *International Journal of Electrochemical Science, 7,* 6154–6167.
19. Firouzi, A., Del Gaudio, C., lamastra, F. R., Montesperelli, G., Bianco, A. (2015). Electrospun polymeric coatings on aluminum alloy as a straightforward approach for corrosion protection. *Journal of Applied Polymer Science, 132(2),* 1–10. DOI 10.1002/app.41250.
20. Li, J., Guan, P., Li, M., Zhang, Y., Cheng, P. et al. (2017). Anticorrosive superhydrophobic polystyrene-coated mesh for continuous oil spill clean-up. *New Journal of Chemistry, 41(12),* 4862–4868. DOI 10.1039/C7NJ00823F.
21. Cui, M., Xu, C., Shen, Y., Tian, H., Feng, H. et al. (2018). Electrospinning superhydrophobic nanofibrous poly (vinylidene fluoride)/stearic acid coatings with excellent corrosion resistance. *Thin Solid Films, 657,* 88–94. DOI 10.1016/j.tsf.2018.05.008.

22. Jadoo, S. A., Naser, J. A. (2020). Adsorption optimization of Congo red dye onto electrospun nanofibers of polyacrylonitrile functionalized with Fe_3O_4 nanoparticles. *IOP Conference Series: Materials Science and Engineering, 928(5),* 052024. DOI 10.1088/1757-899X/928/5/052024.
23. Shaker, A., Abdulrazak, R., Ali, S. A., M, A. (2014). Enhancing of corrosion protection properties using electro-polymerized polyaniline coating. *Archives of Applied Science Research, 6(4),* 243–255.
24. Gaballah, S., Shehata, N., Shaaban, M., Nosier, S., Hefnawy, A. et al. (2017). Corrosion inhibition of aluminum in hydrochloric acid solution using ceria doped polyvinyl chloride nanofiber. *Journal of Electrochemical Science, 12,* 1094–1105. DOI 10.20964/2017.02.05.
25. Wang, H., Liu, Y., Xie, J., Tang, J., Duan, M. et al. (2016). 3-(diethylamino)-1-phenylpropan-1-one as a corrosion inhibitor for N80 steel in acidization of petroleum exploitation. *International Journal of Electrochemical Science, 11,* 4943–4956. DOI 10.20964/2016.06.74.
26. Verma, D. K., Khan, F. (2016). Corrosion inhibition of mild steel in hydrochloric acid using extract of glycine max leaves. *Research on Chemical Intermediates, 42(4),* 3489–3506. DOI 10.1007/s11164-015-2227-7.
27. El-Gendy, N. S., Hamdy, A., Omran, B. A. (2018). Thermal and surface studies on the corrosion inhibition of petroleum pipeline by aqueous extract of allium cepa skin under acidic condition. *Energy Sources, Part a: Recovery, Utilization, and Environmental Effects, 40(8),* 905–915. DOI 10.1080/15567036.2018.1465488.
28. Ansari, K. R., Quraishi, M. A. (2014). Bis-schiff bases of isatin as new and environmentally benign corrosion inhibitor for mild steel. *Journal of Industrial and Engineering Chemistry, 20(5),* 2819–2829. DOI 10.1016/j.jiec.2013.11.014.
29. Shabani-Nooshabadi, M., Ghoreishi, S. M., Behpour, M. (2011). Direct electrosynthesis of polyaniline–montmorrilonite nanocomposite coatings on aluminum alloy 3004 and their corrosion protection performance. *Corrosion Science, 53(9),* 3035–3042. DOI 10.1016/j.corsci.2011.05.053.
30. Hamdy, A., El-Gendy, N. S. (2013). Thermodynamic, adsorption and electrochemical studies for corrosion inhibition of carbon steel by henna extract in acid medium. *Egyptian Journal of Petroleum, 22(1),* 17–25. DOI 10.1016/j.ejpe.2012.06.002.
31. Arshad, N., Singh, A. K., Chugh, B., Akram, M., Perveen, F. et al. (2019). Experimental, theoretical, and surface study for corrosion inhibition of mild steel in 1 M HCl by using synthetic anti-biotic derivatives. *Ionics, 25(10),* 5057–5075. DOI 10.1007/s11581-019-03028-y.